International Journal of Differential Equations and Applications
Volume 14 No. 3 2015, 235-250
ISSN: 1311-2872
url: http://www.ijpam.eu
doi: http://dx.doi.org/10.12732/ijdea.v14i3.2370

acadpubl.eu

ON THE NUMERICAL SIMULATION OF THE VORTEX BREAKDOWN IN THE COMBUSTION PROCESS WITH SIMPLE CHEMICAL REACTION AND AXIAL MAGNETIC FIELD

Harijs Kalis[1], Maksims Marinaki[2 §], Uldis Strautiņš[3], Ojārs Lietuvietis[4]
[1,2,3,4]Institute of Mathematics and Computer Science
University of Latvia
Raiņa bulvāris 29, Rīga LV-1459, LATVIJA

Abstract: The characteristics of a flame are influenced by external magnetic field and the swirl number. The present paper considers a simplified model taking into account the interplay of swirl flow and the MHD effects due to the Lorentz force acting on the weakly ionised gas. We present the results of a numerical study of the viscous, incompressible, laminar, axisymmetric swirling flow in a cylindrical pipe with axial uniform magnetic field. The combustion process is modelled by a single step exothermic chemical reaction of fuel and oxidant. The rate of the reaction is given by one-step first-order Arrhenius kinetics. Fields of stream function, vorticity, temperature, circulation and fuel concentration in the cylindrical pipe are obtained for various values of the uniform axial magnetic field and specific heat of the reaction. The approximations of the nonlinear problems are based on the implicit finite-difference and alternating direction (ADI) methods.

AMS Subject Classification: 65M06, 65N06, 65N22, 35K55, 35K57
Key Words: nonlinear PDE problem, finite–difference, chemical reaction, magnetic field

Received: April 2, 2015

§Correspondence author

1. Introduction

Combustion or burning is a high-temperature exothermic chemical reaction between a fuel and an oxidant producing a flame and releasing heat.

The comprehensive research of the swirling flows with estimation of their applicability to the stabilization and control of fuel combustion started long ago and can be related to the studies of Syred, Gupta and Lilley [1], [2]. These studies analyse the influence of the degree of swirl on the flow dynamics and structure formation in the flame reaction zone. The relevant parameter is the swirl number approximately expressed as the ratio of the average azimuthal and axial velocity components. Vortex breakdown is a critical phenomenon: at a critical swirl number around 0.6 a recirculation zone is formed at the exit of the burner effectively stabilizing the flame and increasing the heat release as the recirculated hot combustion products efficiently ignite the cold fuel - oxidant mixture. At swirl number above 0.6 the formation of a compact recirculation zone is observed. Of particular interest is the influence of external electrical or magnetic fields on the combustion process, see [4]. Experimental data by Zake et al. [4] demonstrate the potential of this approach and refer to the paramagnetic properties of oxygen to explain the observations. The formation of the central recirculation zone under given conditions is unclear and under discussion. Vortex breakdown is a fundamental phenomenon in fluid mechanics and has been studied extensively over the last forty-five years. Axisymmetric flow of a swirling viscous, incompressible fluid jet inside confining cylindrical boundaries has been numerically investigated in [5]. In [6] the vortex breakdown and swirl at the inlet in a longitudinal magnetic field and electric current are obtained. The breakdown zone moves upstream and increases in size with the increase of swirl number. The present paper continues the study of Choi, Rusak et al. [7] by conducting a numerical investigation in cylindrical pipe of the inviscid, axisymmetric, steady swirling flow with axial uniform magnetic field for the low Mach number approximation. Similarly, viscous, incompressible, axisymmetric swirling flow for Reynolds number 100 in cylindrical pipe is considered, using full Navier-Stokes equations. Effects of gravitation are included.

In this paper we consider the interplay of two optimization strategies - inducing swirl in the flows combined by application of an external magnetic field. Swirling the flow at the inlet of the burner has been observed [3] to enhance the mixing of the reactants in the flame reaction zone and stabilize the processes of fuel combustion and heat release. The swirl number is introduced by controlling the axial and azimuthal velocity components at the inlet. Uniform velocity profile is prescribed at the inlet in the radial direction. The azimuthal component is introduced by rotating a part of the boundary. A similar experiment is reported in [3]. The fuel (propane) is injected axially into the sectioned water-cooled channel, swirl motion is generated by a tangential air inlet. The combustion process is lumped in a single exothermic chemical reaction between fuel and oxidant. The rate of the reaction is given by one-step first-order Arrhenius kinetics. In this paper we focus on a configuration in which a steady, low-speed ($0.01\frac{m}{s}$), laminar flame exists in a straight pipe in the base state. Our purpose is to understand how this base state is affected by the introduction of swirl, and how the first appearance of vortex breakdown is influenced by the heat release. This process of the magnetohydrodynamics (MHD) is considered with the so-called inductionless approximation. We model the external axial magnetic field through the Lorentz force term, obtain the dimensionless stationary Navier-Stokes equations, set a computational domain and formulate the system of equations for stream function, vorticity, circulation and temperature fields. The three velocity components, vorticity and temperature have been calculated using the implicit finite difference method, ADI method, under-relaxation and suitable boundary conditions for the vorticity function.

2. The Mathematical Models

A vortex generator is placed upstream for the cylindrical pipe $r' \in [0, r_0], z \in [0, z_0]$ of the inlet $z = 0$. At the outlet the flow exits into the ambient atmosphere. The thermophysical parameters of the fluid are assumed constant. Let U_0, ρ_0, B_0 be the maximum axial speed at the inlet, nominal density and the induction of the axial magnetic field.

Viscous, incompressible (ρ'=constant), axisymmetric flow of the liquid mixture with axial uniform magnetic field in cylindrical pipe is modeled by the dimensional nonstationary Navier-Stokes equations in cylindrical coordinates (r', z) :

$$\begin{cases} \dfrac{1}{r'}\dfrac{\partial(r'u_r)}{\partial r'} + \dfrac{\partial(u_z)}{\partial z} = 0, \\ \dfrac{\partial u_r}{\partial t'} + u_r\dfrac{\partial u_r}{\partial r'} + u_z\dfrac{\partial u_r}{\partial z} - \dfrac{u_\theta^2}{r'} = -\dfrac{1}{\rho}(\dfrac{\partial p'}{\partial r'} + \sigma B_0^2 u_r) + \nu\Delta' u_r, \\ \dfrac{\partial u_\theta}{\partial t'} + u_r\dfrac{\partial u_\theta}{\partial r'} + u_z\dfrac{\partial u_\theta}{\partial z} + \dfrac{u_r u_\theta}{r'} = \nu\Delta' u_\theta, \\ \dfrac{\partial u_z}{\partial t'} + u_r\dfrac{\partial u_z}{\partial r'} + u_z\dfrac{\partial u_z}{\partial z} = -\dfrac{1}{\rho}\dfrac{\partial p'}{\partial z} - \beta_T g(T' - T_0) + \nu\Delta u_z. \end{cases} \tag{1}$$

We consider a single exothermic chemical reaction, in which fuel (F) and oxidant (O_2) combine to produce products (P) and heat. The temperature-dependent rate of the reaction is given by one-step first-order Arrhenius kinetics $K(T') = \exp(-\frac{E}{RT'})$. We have 2-D reaction-diffusion system of two non-linear partial differential equations:

$$\begin{cases} \dfrac{\partial T'}{\partial t'} + u_r \dfrac{\partial T'}{\partial r'} + u_z \dfrac{\partial T'}{\partial z} = \dfrac{\lambda}{\rho c_p} \Delta T' + \dfrac{B}{c_p} A' C' \exp(-\dfrac{E}{RT'}), \\ \dfrac{\partial C'}{\partial t'} + u_r \dfrac{\partial C'}{\partial r'} + u_z \dfrac{\partial C'}{\partial z} = \dfrac{D}{\rho} \Delta C' + A' C' \exp(-\dfrac{E}{RT'}). \end{cases} \tag{2}$$

Here t', r' denote dimensional time and radial coordinates,
u_z, u_r, u_θ - dimensional axial, radial and azimuthal components of the velocity,
$\Delta' q = \Delta q - \frac{q}{r^2}$, $\Delta q = \frac{1}{r'} \frac{\partial}{\partial r'}(r' \frac{\partial q}{\partial r'}) + \frac{\partial^2 q}{\partial z^2}$ is the Laplace operator,
$\nu[\frac{m^2}{s}]$ - kinematic viscosity, $q = T'[K]; C'$ - dimensional temperature and mass fraction of the reactant or the fraction of fuel present,
$\sigma[\frac{1}{\Omega\, m}]$ - electrical conductivity,
$D[\frac{m^2}{s}]$ - molecular diffusivity, $\rho[\frac{kg}{m^3}]$ - density of the fuel,
$\lambda[\frac{J}{s\, m\, K}]$ - thermal conductivity, $c_p[\frac{J}{kg\, K}]$ - specific heat at constant pressure,
$B[\frac{J}{kg}], A'[\frac{1}{s}], E[\frac{J}{mol}]$ - specific heat release, reaction-rate pre-exponential factor and activation energy,
$\beta_T[\frac{1}{K}]$ - volumetric coefficient of thermal expansion,
$g[\frac{m}{s^2}]$ - acceleration due to gravity, $R = 8.314[\frac{J}{mol\, K}]$ - universal gas constant.

The dimensional velocity vector $\vec{U}[\frac{m}{s}]$ is

$$(U_0 w(x,r,t), U_0 u(x,r,t), V_0 v(x,r,t)),$$

where w, u, v are the dimensionless axial, radial and azimuthal velocity components depending on the non-dimensional axial
$x = \frac{z}{z_0} \in [0, x_0], x_0 = \frac{z_0}{r_0}$, radial $r = \frac{r'}{r_0} \in [0,1]$ and time $t = \frac{t'}{r_0/U_0} \in [0, \infty]$.

The dimensional pressure is $p' = p\rho_0 U_0^2$.

The boundary ($r' = r_0$) is subject to heat loss modelled by Newtonian cooling to the ambient surroundings, which is at a temperature $T_0 = 0$ with heat transfer coefficient $h[\frac{J}{s\, m^2\, K}]$. Zero flux of fluid is prescribed, resulting in the boundary conditions

$$\lambda \frac{\partial T'}{\partial r'} = -h(T' - T_0), \quad \frac{\partial C'}{\partial r'} = 0, \; r' = r_0. \tag{3}$$

For the dimensionless parameters $t, r, x, u = \frac{u_r}{U_0}, w = \frac{u_z}{U_0}, v = \frac{u_\theta}{V_0}$, $C = \frac{C' - C_0}{C_0}$, $T = \frac{T' - T_0}{T_w - T_0}$, $A = \frac{A' r_0}{U_0}$ we have following systems (T_w is maximal value of T'):

$$\left\{\begin{array}{l} \dfrac{1}{r}\dfrac{\partial(r,\,u)}{\partial r}+\dfrac{\partial w}{\partial x}=0,\\ \dfrac{\partial u}{\partial t}+u\dfrac{\partial u}{\partial r}+w\dfrac{\partial u}{\partial x}-\Gamma^2\dfrac{v^2}{r}=-\dfrac{\partial p}{\partial r}-Su+\dfrac{1}{Re}\Delta' u,\\ \dfrac{\partial v}{\partial t}+u\dfrac{\partial v}{\partial r}+w\dfrac{\partial v}{\partial x}+\dfrac{u\,v}{r}=\dfrac{1}{Re}\Delta' v,\\ \dfrac{\partial w}{\partial t}+u\dfrac{\partial w}{\partial r}+w\dfrac{\partial w}{\partial x}=-\dfrac{\partial p}{\partial x}-\dfrac{Gr}{Re^2}T+\dfrac{1}{Re}\Delta w \end{array}\right. \tag{4}$$

and

$$\left\{\begin{array}{l} \dfrac{\partial T}{\partial t}+u\dfrac{\partial T}{\partial r}+w\dfrac{\partial T}{\partial x}=P_1\Delta T+\beta A\,C\exp(-\dfrac{\delta}{T}),\\ \dfrac{\partial C}{\partial t}+u\dfrac{\partial C}{\partial r}+w\dfrac{\partial C}{\partial x}=P_2\Delta C-A\,C\exp(-\dfrac{\delta}{T}), \end{array}\right. \tag{5}$$

where $P_1=\frac{Le}{Pe}, P_2=\frac{1}{Pe}, Pe=\frac{\rho U_0 r_0}{D}, Le=\frac{\lambda}{c_p\,D}$ are Péclet and Lewis numbers, $\Gamma=\frac{V_0}{U_0}$ is the swirl number (V_0 - maximal value of the azimuthal velocity), $\beta=\frac{B}{c_p\,T_0}$ is the heat release parameter, $\delta=\frac{E}{R\,T_0}$ - the scaled activation energy, $Re=\frac{U_0 r_0}{\nu}, S=\frac{\sigma B_0^2\,r_0}{\rho\,U_0},\ Gr=\frac{\beta_t g(T_w-T_0)r_0^3}{\nu^2}$ are Reynolds, Stewart and Grashof numbers.

The dimensionless boundary condition for temperature on $r=1$ is

$$\frac{\partial T}{\partial r}+Bi(T-1)=0,$$

where $Bi=\frac{h\,r_0}{\lambda}$ is the Biot number.

The other BCs are following:

1) along the pipe axis $r=0:\ u=v=0, \frac{\partial T}{\partial r}=\frac{\partial C}{\partial r}=\frac{\partial w}{\partial r}=0$ (the symmetry conditions),

2) at the pipe wall $r=1:\ u=v=w=0, \frac{\partial T}{\partial r}=\frac{\partial C}{\partial r}=0,$

3) at the pipe outlet $x=x_0:\ u=0,\ \frac{\partial T}{\partial x}=\frac{\partial C}{\partial x}=\frac{\partial w}{\partial x}=\frac{\partial v}{\partial x}=0,$

4) at the pipe inlet $x=0:\ u=0$ for $r\in[0,1]$;

$$w=1,\ T=1,\ C=1-\frac{r^2}{r_1^2},\ v=0$$

for $r\in[0,r_1]$;

$$w=0,\ T=0.5,\ C=0,\ v=4\frac{(r-r_1)(1-r)}{(1-r_1)^2}$$

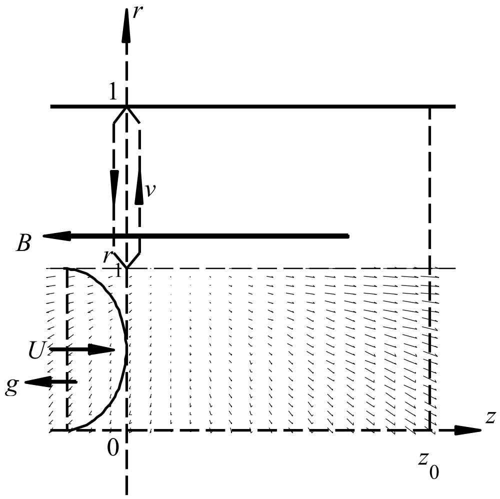

Figure 1: Computational domain

for $r \in [r_1, 1]$.

Thus we prescribe uniform jet flow for $r < r_1$ and rotation for $r > r_1$ with maximal speed 1 (see Fig. 1).

For obtaining the unknown functions p, T, C, u, w, v, the system of 6 equations (4) and (5) is used. We seek the steady solution as the time asymptotic limit of the solutions of the unsteady equations.

3. The Equations for Numerical Simulation

For numerical solution we eliminate the pressure from the equations by introducing the stream function Ψ and vorticity ζ with following expressions:

$$rw = \frac{\partial \Psi}{\partial r}, \quad ru = -\frac{\partial \Psi}{\partial x}, \quad \zeta = \frac{\partial u}{\partial x} - \frac{\partial w}{\partial r}.$$

From (4) we have the following system of equations:

$$\begin{cases} \dfrac{\partial \zeta}{\partial t} + u\dfrac{\partial \zeta}{\partial r} + w\dfrac{\partial \zeta}{\partial x} - \dfrac{u\,\zeta}{r} = \dfrac{\Gamma^2}{r}\dfrac{\partial v^2}{\partial x} + \dfrac{1}{Re}\Delta'\zeta - S\dfrac{\partial u}{\partial x} + \dfrac{Gr}{Re^2}\dfrac{\partial T}{\partial r}, \\ \dfrac{\partial \Psi}{\partial t} = \dfrac{\partial^2 \Psi}{\partial x^2} + r\dfrac{\partial}{\partial r}(r^{-1}\dfrac{\partial \Psi}{\partial r}) + r\zeta, \end{cases} \tag{6}$$

where the second equation for numerical simulation is transformed to nonsteady. In order to remove the source terms $\frac{u\,v}{r}, \frac{u\,\zeta}{r}$, we use the transformation

$\tilde{v} = vr$ (the circulation) and $\tilde{\zeta} = \frac{\zeta}{r}$ (modified vorticity) [6]. Therefore we obtain following equations:

$$\begin{cases} \dfrac{\partial\tilde{\zeta}}{\partial t} + u\dfrac{\partial\tilde{\zeta}}{\partial r} + w\dfrac{\partial\tilde{\zeta}}{\partial x} = \dfrac{\Gamma^2}{r^4}\dfrac{\partial\tilde{v}^2}{\partial x} + \dfrac{1}{Re}(\dfrac{\partial^2\tilde{\zeta}}{\partial x^2} + \dfrac{1}{r^3}\dfrac{\partial}{\partial r}(r^3\dfrac{\partial\tilde{\zeta}}{\partial r})) - \dfrac{S}{r}\dfrac{\partial u}{\partial x} + \dfrac{Gr}{r\,Re^2}\dfrac{\partial T}{\partial r}, \\ \dfrac{\partial\Psi}{\partial t} = \dfrac{\partial^2\Psi}{\partial x^2} + r\dfrac{\partial}{\partial r}(r^{-1}\dfrac{\partial\Psi}{\partial r}) + r^2\tilde{\zeta}, \\ \dfrac{\partial\tilde{v}}{\partial t} + u\dfrac{\partial\tilde{v}}{\partial r} + w\dfrac{\partial\tilde{v}}{\partial x} = \dfrac{1}{Re}(\dfrac{\partial^2\tilde{v}}{\partial x^2} + r\dfrac{\partial}{\partial r}(r^{-1}\dfrac{\partial\tilde{v}}{\partial r})). \end{cases} \tag{7}$$

For flow we use following BCs:

1) along the axis $r = 0:\ \tilde{v} = 0,\ \Psi = 0,\ \frac{\partial\tilde{\zeta}}{\partial r} = 0,$

2) at the wall $r = 1:\ \tilde{v} = 0,\ \Psi = q, \tilde{\zeta} = \zeta_w(x),$

3) at the pipe outlet $x = x_0:\ \frac{\partial\tilde{\zeta}}{\partial x} = \frac{\partial\Psi}{\partial x} = \frac{\partial\tilde{v}}{\partial x} = 0,$

4) at the pipe inlet $x = 0:\ \Psi = 0.5r^2,\ \tilde{v} = 0,\ \tilde{\zeta} = 0$ for $r \in [0, r_1]$ and $\Psi = q,\ \tilde{v} = 4r\frac{(r-r_1)(1-r)}{(1-r_1)^2},\ \tilde{\zeta} = 0$, for $r \in [r_1, 1]$. Here $q = \frac{r_1^2}{2}$ is the dimensionless fluid volume, $\zeta_w(x)$ is the boundary value of vorticity, obtained by an iterative process, see [8]:

$$\zeta_w^k(x) = \omega\frac{\partial\Psi}{\partial r} + \zeta_w^{k-1}(x),\ k = 1, 2, \ldots,$$

where k is iteration index and $\zeta_w^0(x) = 0$, $\omega > 0$ a relaxation parameter.

The initial conditions are computed by multiplying BCs at $x = 0$ with $\exp(-x)$.

4. The Numerical Approximations and the Stationary 1D Reaction-Diffusion Problem

We use the uniform grid in space with $(M + 1) \times (N + 1)$ points:

$$\{(r_i, x_j),\ \ r_i = (i-1)h_r,\ \ x_j = (j-1)h_x,\ \ i = \overline{1, M+1},\ \ j = \overline{1, N+1}\},$$

$M \cdot h_r = 1, M_1 \cdot h_r = r_1, N \cdot h_x = x_0$, and uniform time grid $t_n = n\tau$, $n = 0, 1, \ldots$. A function $U(t, r, x)$ is approximated with the grid function taking values $U_{i,j}^n \approx u(t_n, r_i, x_j)$.

For the approximation in space we use the central differences and the implicit differences in time. For solving 2D discrete problem in time

$$(U^{n+1} - U^n)/\tau = (\Lambda_x + \Lambda_x)U^{n+1} + f^n, n \geq 0,$$

we use ADI method from Douglas and Rachford (1955) in the form

$$(U^{n+0.5}-U^n)/\tau = \Lambda_x U^{n+0.5}+\Lambda_x U^n+f^n, \quad (U^{n+1}-U^{n+0.5})/\tau = \Lambda_r(U^{n+1}-U^n),$$

where $U^{n+0.5}$ and U^{n+1} are obtained with Thomas algorithm in x and r directions respectively.

Eliminate the half time step and we obtain the previous discrete problem with approximation error $O(\tau^2)$. Here Λ_x, Λ_r are differential operators, containing first and second order derivatives with respect to x and r, f^n are other functions and derivatives in the PDE. For solution of the stationary 1D problem for reaction-diffusion equations (5)

$$(w = \text{const}, u = 0, T = T(x), C = C(x), x \in [0, 2])$$

and BCs

$$T(0) = C(0) = 1, \ \frac{\partial T(2)}{\partial x} = \frac{\partial C(2)}{\partial x} = 0,$$

we use the Matlab solver `bvp4c`.

For $w = 0$ we multiply the second equation with β and sum both equations to obtain the equation $P_1 T''(x) + P_2 \beta C''(x) = 0$ or $P_1(T(x) - 1) + P_2\beta(C(x) - 1) = 0$.

For $w = 1, A = 50000, \beta \in [0.1, 1], P_1 = P_2 = 0.1, \delta = 10$, the results are represented in Figs 2, 3.

In the case for $w = 1, P_1 = P_2 = 0.1$ we have equation

$$P_1 w(T' + \beta C') = T'' + \beta C''.$$

If $x \to 2$, then $T'' + \beta C'' \to 0$ and $(T - 1) + \beta(C - 1) \to 0$.

If $C \to 0$, then $T \to 1 + \beta = T(2) = \max(T(x))$.

In the Table 1 the maximal temperatures $MT = T_{max} = T(2)$ are shown and the derivatives $T'(0), C'(0)$ for $\beta = \beta_1 \in [0.1, 0.9]$; $\beta = \beta_2 \in [2, 10]$ are obtained with $[90 \div 3000]$ grid points via Matlab solver `bvp4c` with `RelTol = 1.0e-10, Nmax =15000`.

Using discrete approximation for $\beta = 0.1, \ \tau = 1, \ w = 1$ we have the solutions $T(2) = 1.0999, \ C(2) = 0.0010$ with $N = 80, \ iT = 200$, where iT is the number of iterations or time steps. Newton iterations give similar results. For 1D problem we obtain, that the increase in heat of reaction β leads to increase in maximal velocity and decrease in thickness of the boundary layers for temperature and concentration when $x = 0$. We obtain also, that the increase in the axial velocity w for $Le > 1$ rises the increase (for $Le < 1$ - decrease) in maximal temperature of reaction. Increase in w leads to decrease in thickness of boundary layers for concentration for every Le and $x = 0$; when $Le = 1$, the maximal temperature does not depend on w.

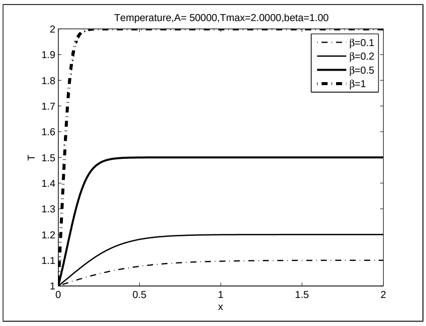

Figure 2: Temperature for $\beta = 0.1; 0.2; 0.5; 1.0$

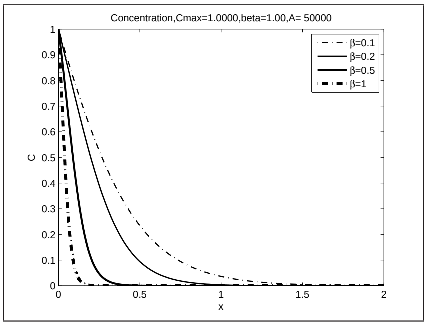

Figure 3: Fraction of fuel for $\beta = 0.1; 0.2; 0.5; 1.0$

4.1. The 2D Reaction-Diffusion Problem

Using alternating-direction implicit (ADI) method for 2D reaction-diffusion equation ($A = 50000, \delta = 10, Bi = 0.1, \beta = 0.5; 5, P_1 = P_2 = 0.1, w = 1, u = 0, \tau = 0.001, It = 20000$) we obtain the following results (for the iterative process we use maximal error $\leq 10^{-5}$; the rate of reaction is calculated as $R = AC\exp(\delta/T)$):1) $\beta = 0.5$, $T \in [0.194, 1.244], \max R = 5.34$ (see Figs 4, 5).

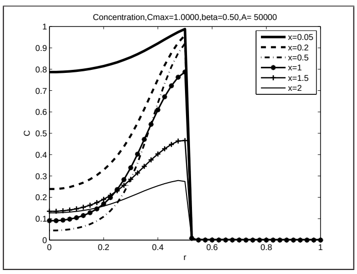

Figure 4: Profile fraction of fuel for x=const by $\beta = 0.5$

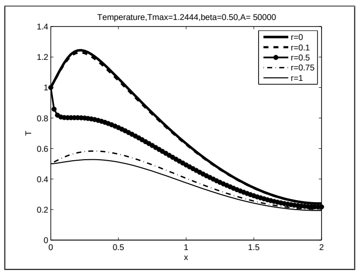

Figure 5: Profile of temperature for r=const by $\beta = 0.5$

2) $\beta = 5$, $T \in [0.188, 5.928], \max R = 173.47$ (see Figs 6,7).

5. Some Numerical Results for Full 2D Problem

The characteristic length scale is $r_0 = 0.05m$, magnitude of the uniform axial and azimuthal velocities $U_0 = V_0 = 0.01\frac{m}{s}$, kinematic viscosity $\nu = (5 \cdot 10^{-6} \ldots 5 \cdot 10^{-5})[\frac{m^2}{s}]$, electrical conductivity for liquid mixture $\sigma = (0 \ldots 100)[\frac{1}{\Omega\, m}]$,

Table 1: The maximal temperature $MT = T_{max}$ and derivatives $T'(0), C'(0)$

β_1	MT	$T'(0)$	$C'(0)$	β_2	MT	$T'(0)$	$C'(0)$
0.1	1.0999	0.21	−2.15	1	2.000	14.76	−14.76
0.2	1.200	0.51	−2.54	2	3.000	126	−63
032	1.300	0.94	−3.15	3	4.000	343	−114
0.4	1.4000	1.62	−4.05	4	5.000	626	−157
0.5	1.5000	2.62	−5.26	5	6.000	953	−191
0.6	1.6000	4.04	−6.74	6	7.000	1310	−218
0.7	1.7000	5.93	−8.47	7	8.000	1687	−241
0.8	1.8000	8.32	−10.40	8	9.000	2079	−260
0.9	1.9000	11.25	−12.51	9	10.00	2479	−275
1.0	2.000	14.76	−14.76	10	11.00	2886	−289

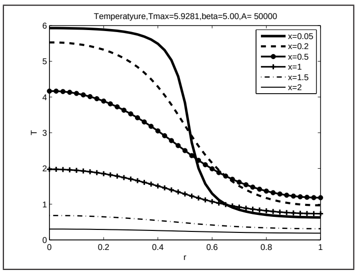

Figure 6: Profile of temperature for x=const by $\beta = 5$

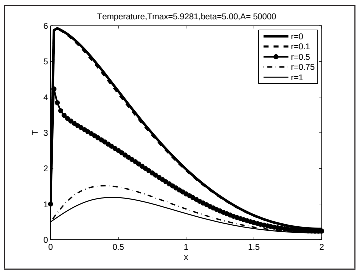

Figure 7: Profile of temperature for r=const by $\beta = 5$

molecular diffusivity $D = 5 \cdot 10^{-5}[\frac{m^2}{s}]$, density $\rho = (1 \ldots 10)[\frac{kg}{m^3}]$, thermal conductivity $\lambda = (0.1 \ldots 1)[\frac{J}{s\,m\,K}]$, specific heat at constant pressure $c_p = 1 \cdot 10^3[\frac{J}{kg\,K}]$, specific heat release $B = (0.5 \cdot 10^6 \ldots 5 \cdot 10^6)[\frac{J}{kg}]$, reaction-rate pre-exponential factor $A' = 1 \cdot 10^4[\frac{1}{s}]$, activation energy $E = 8 \cdot 10^4[\frac{J}{mol}]$, acceleration due to gravity $g = 10[\frac{m}{s^2}]$, volumetric coefficient of thermal expansion $\beta_T = 2 \cdot 10^{-4}[\frac{1}{K}]$, heat transfer coefficient $h = 2[\frac{J}{s\,m^2\,K}]$, initial temperature $T_0 = 300[K], T_w = 1300[K]$, initial mass fraction of the reactant $C_0 = 2[\frac{mol}{m^3}]$. The applied magnetic field is $B_0 = \sqrt{S/50} \in [0, 0.45][T], S \in [0, 10]$.

For modelling, we chose the following parameters: $Re = 100,\ S = 0; 10;\ Gr = 0; 100000, \Gamma = 0; 1; 3; 5,\ x_0 = 2; 4, r_1 = 0.5,\ P_1 = P_2 = 0.1,\ \beta = 0.5; 5,\ \delta = 10,\ A = 50000, Bi = 0.1,\ \tau = 0.001; 0.0001,\ It = 20000 \div 40000,\ N = 80,\ M =$

40.

For flow with $Gr = 0,\ \Gamma = 1,\ S = 0,\ \beta = 5,\ x_0 = 4$, we obtain the following results: $\max V = 1.1399,\ \max T = 5.9331,\ \zeta \in [-2.63, 3.91]$; if $x_0 = 2$ then $\max V = 1.140,\ \max T = 5.933,\ \zeta \in [-2.62, 3.90]$; if $x_0 = 2,\ N = 160,\ M = 40$, then $\max V = 1.1309, \max T = 5.952,\ \zeta \in [-2.64, 3.88]$. In Figs. 8-11 we present the stream function, profile of temperature and axial velocity for $\Gamma = 1,\ S = 0; 10,\ Gr = 0,\ \beta = 5,\ x_0 = 4$. In Figs. 12-21 – the stream function, profile of temperature and axial velocity for $\Gamma = 3; 5,\ S = 0; 10,\ Gr = 10^5,\ \beta = 0.5,\ x_0 = 2$. The results of calculations are given in Table 2.

Table 2: The values of $\beta, \Gamma, S, \max U, \max R, \max T, \max|\zeta|, \min\Psi, Gr, x_0$

β	Γ	S	$maxU$	$maxR$	$maxT$	$max\|\zeta\|$	$min\Psi$	Gr	x_0
0.5	1	0	1.00	7.296	1.359	4	0	0	2
5	1	0	1.140	173.1	5.933	4	0	0	2
5	1	0	**1.140**	173.1	**5.932**	4	0	0	4
5	1	10	**1.059**	173.7	**5.948**	6	0	0	4
5	1	0	3.296	169.4	5.616	112	-0.24	$1.e+5$	4
5	1	0	**3.274**	169.17	**5.599**	111	-0.24	$1.e+5$	2
5	1	10	**2.445**	170.81	**5.764**	46	-0.11	$1.e+5$	2
0.5	3	0	**1.837**	2.677	**1.0437**	16	-0.066	$1.e+5$	2
0.5	3	10	**1.409**	6.707	**1.317**	20	-0.010	$1.e+5$	2
0.5	5	0	**1.970**	2.671	**1.0433**	68	-0.055	$1.e+5$	2
0.5	5	10	**1.438**	6.16	**1.310**	39	-0.011	$1.e+5$	2
5	0	0	1.088	173.13	5.936	2	0	0	2
5	3	0	**1.265**	172.92	**5.924**	22	0	0	2
5	3	10	**1.00**	173.70	**5.948**	14	0	0	2
0.5	3	0	**1.265**	7.083	**1.342**	22	0	0	2
0.5	3	10	**1.00**	7.660	**1.376**	14	0	0	2
5	5	0	**1.606**	172.86	**5.920**	50	0	0	2
5	5	10	**1.095**	173.65	**5.947**	35	0	0	2
0.5	5	0	**1.606**	6.941	**1.333**	50	0	0	2
0.5	5	10	**1.095**	7.658	**1.376**	35	0	0	2

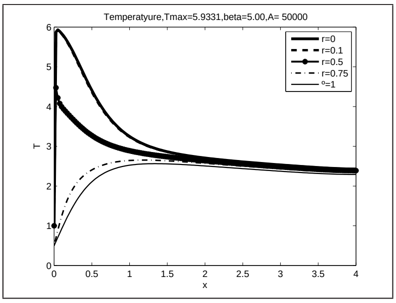

Figure 8: Profile of temperature T for r=const by $\Gamma = 1, S = 0, Gr = 0, \beta = 5, x_0 = 4$

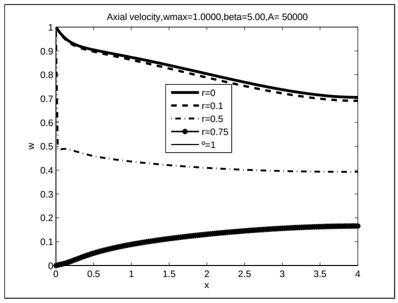

Figure 9: Profile of axial velocity w for r=const, $\Gamma = 1, S = 10, Gr = 0, \beta = 5, x_0 = 4$

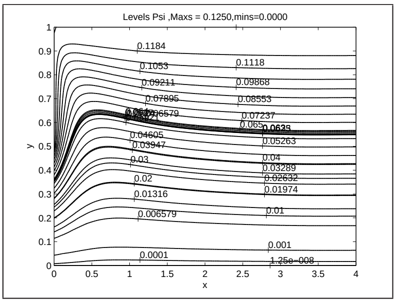

Figure 10: Stream function for $\Gamma = 1, S = 0, Gr = 0, \beta = 5, x_0 = 4$

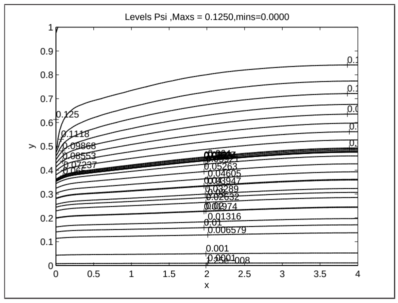

Figure 11: Stream function for $\Gamma = 1, S = 10, Gr = 0, \beta = 5, x_0 = 4$

6. Conclusions

- The flow fields are influenced by gravitation, magnetic field, heat of reaction and swirl number.

- With gravitation ($Gr = 100000$) and $S = 0, \Gamma > 0$ the inlet flow is deflected towards the wall forming a prominent vortex that blocks the central part of the pipe. This effect is diminished by an external magnetic field (S=10) so that the vortex travels downstream, leading to a more uniform velocity distribution.

- External magnetic field ($S = 10$) decreases the maximal velocity while increasing the temperature and rate of reaction.

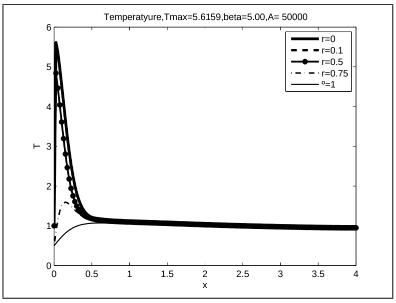

Figure 12: Profile of temperature T for r=const by $\Gamma = 1, S = 0, Gr = 10^5, \beta = 5, x_0 = 4$

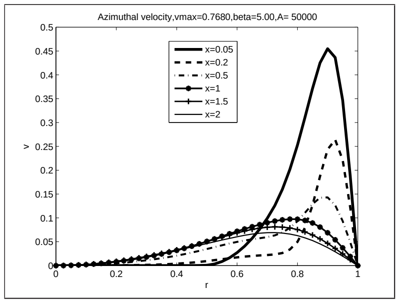

Figure 13: Profile of circulation for x=const by $\Gamma = 3, S = 10, Gr = 10^5, \beta = 0.5, x_0 = 2$

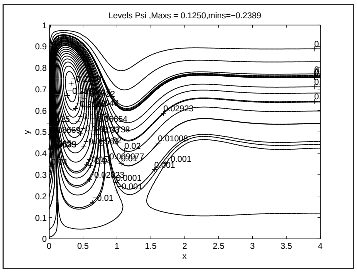

Figure 14: Stream function for $\Gamma = 1, S = 0, Gr = 10^5, \beta = 5, x_0 = 4$

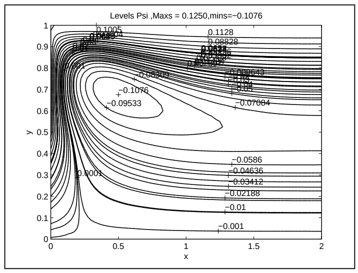

Figure 15: Stream function for $\Gamma = 1, S = 10, Gr = 10^5, \beta = 5, x_0 = 2$

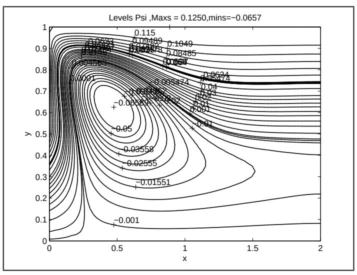

Figure 16: Stream function for $\Gamma = 3, S = 0, Gr = 10^5, \beta = 0.5, x_0 = 2$

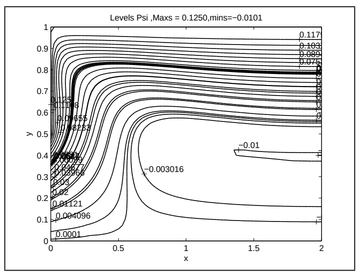

Figure 17: Stream function for $\Gamma = 3, S = 10, Gr = 10^5, \beta = 0.5, x_0 = 2$

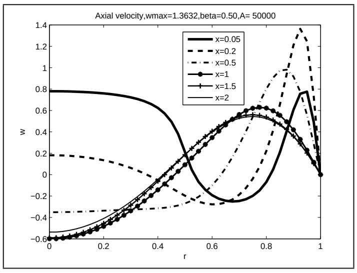

Figure 18: Profile of axial velocity w for x=const by $\Gamma = 5, S = 0, Gr = 10^5, \beta = 0.5, x_0 = 2$

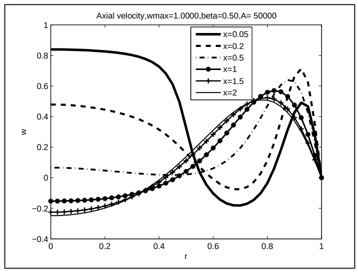

Figure 19: Profile of axial velocity w for x=const by $\Gamma = 5, S = 10, Gr = 10^5, \beta = 0.5, x_0 = 2$

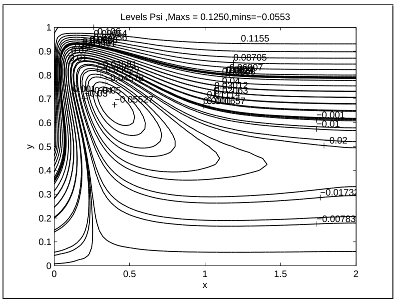

Figure 20: Stream function for $\Gamma = 5, S = 0, Gr = 10^5, \beta = 0.5, x_0 = 2$

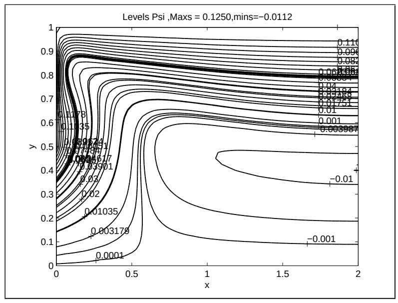

Figure 21: Stream function for $\Gamma = 5, S = 10, Gr = 10^5, \beta = 0.5, x_0 = 2$

- Increase in the heat of reaction β leads to increase in the maximal velocity, temperature and rate of reaction.
- Increase in swirl number Γ leads to increase in the maximal velocity and decrease in temperature and rate of reaction.
- The MHD mechanisms considered in the present study can lead to the increase in temperature by a few percent under application of a strong magnetic field. Since the conductivity of hot gases such as air, oxygen, hydrogen is very low, this mechanism is not very effective in practical applications of gas combustion. Maximal temperature is much more sensitive w.r.t. other parameters such as the specific heat release β than w.r.t. magnetic field. This is in contrast with conductive liquids, for which external magnetic field can be effectively used to control the vorticity distribution in the flow, e.g., to decrease the vorticity in a swirling

flow.

- The distribution of oxygen is strongly influenced by its paramagnetic properties, leading to transport towards stronger magnetic field intensities [4]. This effect will be included in subsequent simulations.

Acknowledgments

Authors gratefully acknowledge the partial support from the grant Nr. 623/2014 of the Latvian Council of Science.

References

[1] N. Syred, J.M. Beer, Combustion in Swirling Flows: A review, *Combustion and Flame*, **23** (1974), 143-201.

[2] D.G. Lilley, Swirl flows in combustion: A review, *AIAA Journal*, **15**, No. 8 (1977), 1763-1778.

[3] M. Zake, I. Barmina, M. Lubane, Swirling Flame. Part 1. Experimental study of the effect of stage combustion on soot formation and carbon sequestration from the nonpremixed swirling flame, *Magnetohydrodynamics*, **40**, No. 2 (2004), 161-181.

[4] M. Zake, I. Barmina, I. Bucenieks, V. Krishko, Magnetic field control of combustion dynamics of the swirling flame flow, *Magnetohydrodynamics*, **46**, No. 2 (2004), 171-186.

[5] J.P. Narain, Numerical prediction of confined swirling jets, *Computers and Fluid*, **5** (1977), 115-125.

[6] Kh.E. Kalis, Yu.B. Kolesnikov, N.N. Polyakov, A rotations flow in a longitudinal magnetic field, *Magnetohydrodynamics*, **19**, No. 1 (1983), 57-61.

[7] J.J. Choi, Z. Rusak, A.K. Kapila, Numerical simulation of premixed chemical reactions with swirl, *Combustion theory and modelling*, **6**, No. 11 (2007), 863-887.

[8] A.A. Dorodnicyn, N.A. Meller, On certain approaches to the solution of the stationary Navier-Stokes equations, *Z*h. Vychisl. Mat. Mat. Fiz., **8** (1968), 393-402.